A&A 376, 402–412 (2001)
DOI: 10.1051/0004-6361:20011003

Astronomy & Astrophysics

Centaurus A: Molecular gas shells or large-scale outflow?⋆

S. J. Curran[1,2,3,⋆⋆]

[1] Onsala Space Observatory, Chalmers University of Technology, 439 92 Onsala, Sweden
[2] School of Physics, University of New South Wales, Sydney NSW 2052, Australia
[3] European Southern Observatory, Casilla 19001, Santiago 19, Chile

Received 2 May 2001 / Accepted 6 July 2001

Abstract. In order to test if the molecular "shells" observed by Charmandaris et al. (2000) could be due to a molecular outflow, we have mapped CO in $J = 1 \rightarrow 0$ and $2 \rightarrow 1$ along the jet axis of Centaurus A. Where our map coincides with their observed positions, like them, we obtain 4σ detections with a similar antenna temperature for CO $1 \rightarrow 0$, although both transitions appear to be somewhat wider in velocity dispersion than theirs. As well as these, we have several tentative detections at distances of $\gtrsim$5 kpc from the nucleus, and although these results are of too poor quality in order to verify or refute the shell model in favour of a molecular outflow, our observations of the inner kpc do suggest that at least a small-scale outflow is a possibility. Whether this would be a component of a larger-scale outflow or exists in conjunction with the molecular gas shells will have to wait for a much more extensive mapping of the large-scale gas distribution in Centaurus A, for which these and the results of Charmandaris et al. (2000) will hopefully provide sufficient motivation.

Key words. galaxies: active – galaxies: jets – galaxies: Seyfert – galaxies: individual: Centaurus A – galaxies: kinematics and dynamics – galaxies: structure

1. Introduction

At a distance of 3 Mpc, Centaurus A (NGC 5128) is the closest giant elliptical galaxy as well as being a powerful source of radio continuum, far infrared and X-ray emission (in fact it is the brightest 100 keV extragalactic source). Recently, Charmandaris et al. (2000) have observed, in CO, regions of molecular gas located at ≈15 kpc along the direction of the strong radio lobes/jets (Clarke et al. 1992), Fig. 1. The authors attribute the molecular gas in these locations to the shells of gas believed to result from the consumption of a companion galaxy in early type systems: While the diffuse atomic gas at these distances is expected to lose its energy and thus fall toward the gravitational centre, the authors suggest that much denser ($\sim 10^3$ cm^{-3}) molecular clouds may be expected to survive at these locations. Looking at Fig. 1, however, one cannot help but notice several similarities to the Circinus galaxy:

1. The location of the outlying molecular gas appears to be aligned with the jet/ionisation cone (Clarke et al. 1992; Rydbeck et al. 1993; Curran et al. 1999) present in both galaxies (Figs. 1 and 2). The ionisation cone in Centaurus A is possibly observed to the NE by Bryant & Hunstead (1999)[1]: In Circinus the NW portion of the cone is observed which corresponds to the approaching segment, while the receding is believed to be obscured by the galactic disk (Curran et al. 1999, and references therein);
   As well as this:
2. Both galaxies contain a fast (≈200 km s^{-1}) rotating 100-pc scale ring of molecular clouds whose axis coincides with that of the jet, i.e. the outlying gas is orientated along the minor axis of the ring (Rydbeck et al. 1993; Curran et al. 1998, 1999; Marconi et al. 2001), Figs. 1 and 2;
3. Finally, CO has also been detected at a similar antenna temperature (Fig. 1) as far as 1.2 kpc along the minor axis (i.e. outflow axis) of Circinus (Curran et al. 2001b).

From these points we felt that the molecular gas distribution warranted further investigation. In order to determine whether the outlying CO could be due to a molecular outflow rather than a shell of molecular clouds, we performed a more complete map of the CO along the jet/lobe direction in Centaurus A and present our results in this paper.

⋆ Based on results collected at the European Southern Observatory, La Silla, Chile.

⋆⋆ e-mail: sjc@bat.phys.unsw.edu.au

[1] Although Hα + [NII] (cf. Fig. 2) have been observed in Centaurus A (e.g. Phillips et al. 1986), due to the high level of obscuration by dust, no such image exhibiting the ionisation cone is available. Instead this is inferred from the conical morphology of the hot dust emission (Bryant & Hunstead 1999).

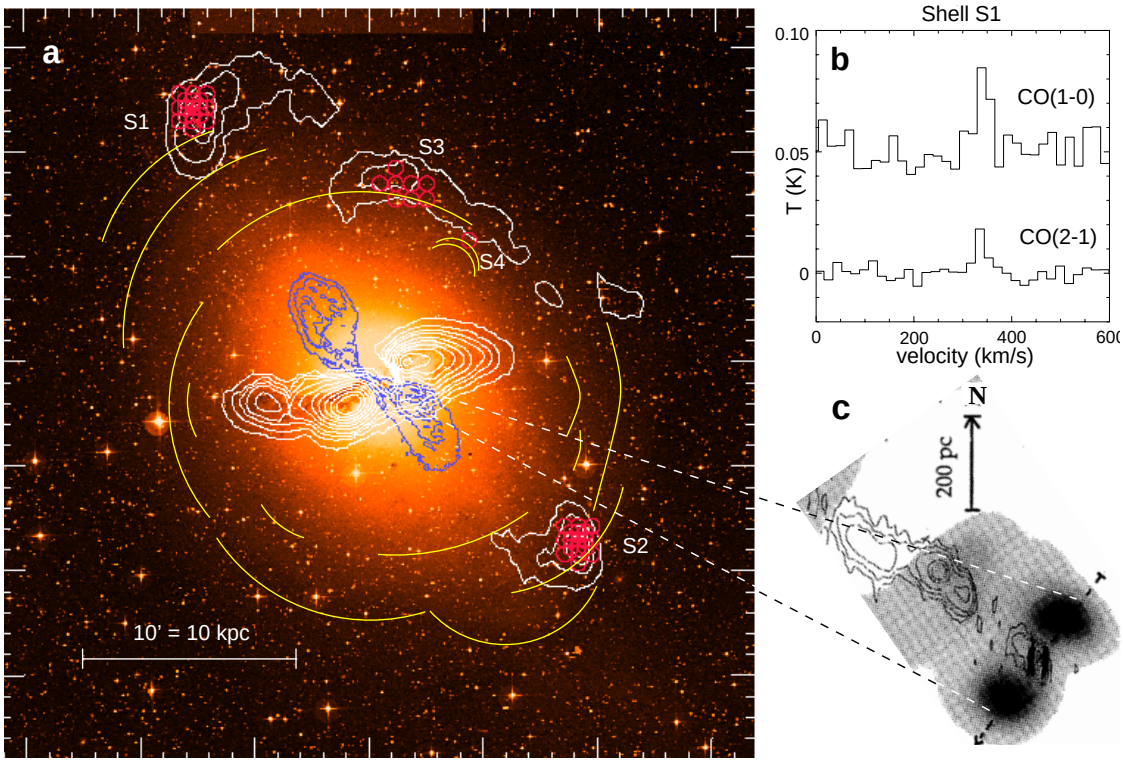

Fig. 1. a) A Digitised Sky Survey optical image of Centaurus A with the contours of HI gas superimposed in white. The darker contours show the radio lobes (see below) and positions S1 and S2 show the location of the CO 1 → 0 and 2 → 1 detections (no CO was detected towards S3 or S4), an example is shown in **b)**. **c)** The deconvolved CO 2 → 1 map of highly blue and red-shifted gas of Rydbeck et al. (1993) superimposed upon the 1.5 GHz VLA image of the radio jet (Burns et al. 1983). Adapted from Charmandaris et al. (2000) and Rydbeck et al. (1993) courtesy of Vassilis Charmandaris and Gustaf Rydbeck.

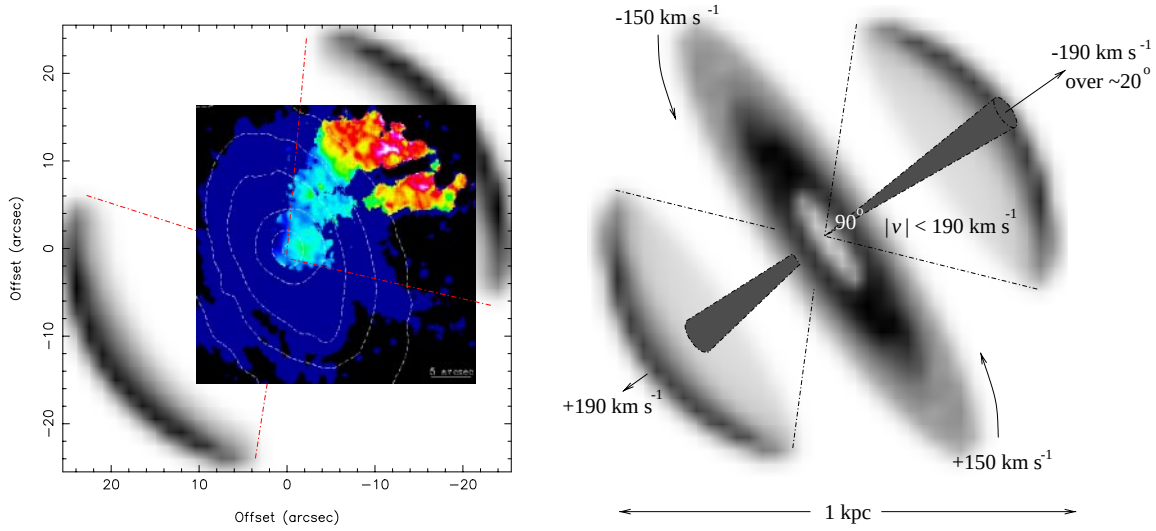

Fig. 2. Left: The ionisation cone in Circinus (Marconi et al. 1994) scaled and superimposed upon the molecular outflow of Curran et al. (1999). [OIII]/(Hα + [NII]) image courtesy of Ernesto Oliva. Right: The CO distribution (molecular outflow+ring) within the centre of Circinus (Curran et al. 1999). The possible high velocity outflow component (which coincides with the jet) is shown. Taken from Curran (2000b).

2. Observations

The observations were performed in February 2001 with the 15 m SEST at La Silla, Chile[2] with the 115 & 230 GHz (IRAM) receivers. The receivers were tuned to single-sideband mode and typical system temperatures, on the $T_{\rm A}^*$-scale, were around 500 K for both receivers.

[2] The Swedish-ESO Sub-millimetre Telescope is operated jointly by ESO and the Swedish National Facility for Radio Astronomy, Onsala Space Observatory, Chalmers University of Technology.

The backends were acousto-optical spectrometers with 1440 channels and a channel width of 0.7 MHz. We used dual-beam switching with a throw of about 12′ in azimuth, and pointing errors were typically 3″ rms on each axis. The intensity was calibrated using the chopper-wheel method. For all of the observing runs the weather was clear, although, as usual for this time of year, the humidity was higher than would have been preferred, resulting in the higher system temperatures. Only linear baselines were removed.

3. Results and discussion

3.1. The map

In order to determine how the CO varies along the jet direction (PA = 51° for the inner lobes, Clarke et al. 1992) we mapped along a single strip at this position angle (roughly) extending between S1 and S2[3] at 44″ (one CO 1 → 0 beam) spacing. This strip was selected as we wished to concentrate on the (stronger) NE jet/ionisation cone. In order to obtain a more complete picture of any cone structure, we also mapped in single strips perpendicular to the axis at 5, 10 and 15 kpc along the axis, Fig. 3. Assuming a conical angle of 60° (Bryant & Hunstead 1999)

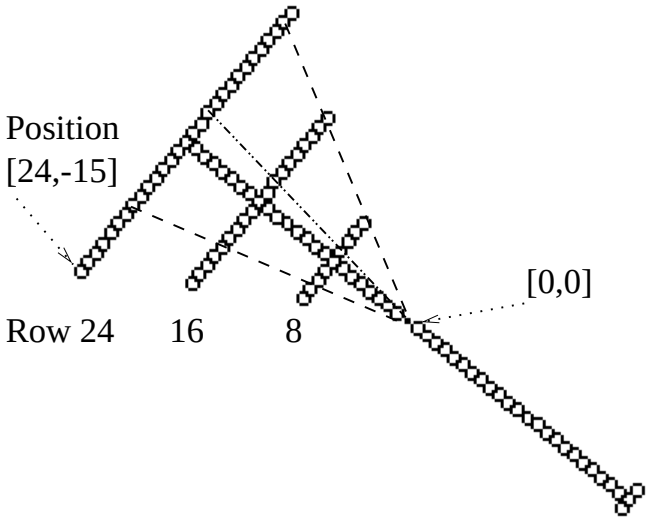

Fig. 3. The positions mapped. The dashed lines represent hypothesised cone edges and the dashed/dotted line the hypothesised axis (see Sect. 3.4).

lead to us adding a further 56 positions to the 50 axis positions. Two further were added at the extreme SW face raising the total to 106 map positions (although, as mentioned above, this results in a 4.5 kpc deviation from position S2). Note that, due to the accidental addition of one more position, this actually comes to 107. The maps are shown in Figs. 4 and 5.

For the observations we found it useful to refer to the map positions in a vectorial fashion, e.g. [24,−15] is 24 positions "up" (NE) along the jet axis (Fig. 1) and −15 "down" along the face, that is, the position farthest left in Fig. 3 or position (670, 1056) in Figs. 4 and 5. We use this notation in the remainder of the paper.

[3] Although by doing this we actually miss S2 by around 20°, Fig. 1.

Table 1. The integrated main-beam line intensities at various offsets along row 24 of the map (Fig. 3). In this and Tables 3, 4 and 5 the top and middle rows denote the CO 1 → 0 and 2 → 1 values [K km s^{-1}], respectively (the uncertainties are due to 1σ rms noise fluctuations), and the third row denotes the approximate central velocity (l.r.s.) of the line [km s^{-1}].

−15	−14	−13	−12	−11	−10
<2	<4	<4	<4	<4	3.1(0.6)
3.0(1.5)	<1	1.0(0.3)	1.0(0.5)	1.7(0.4)	<1
700	–	700	350	350	300
−9	−8	−7	−6	−5	−4
<4	1.2(0.5)	<4	<4	<4	<4
<0.6	0.7(0.2)	<0.5	<0.5	1.2(0.5)	<0.9
–	500	–	–	500	–
−3	−2	−1	0	1	2
<4	2.1(0.4)	<4	<6	3.6(1.3)	1.4(0.7)
<0.9	<0.8	<0.8	<0.8	<0.9	<0.9
–	650	–	–	150	200
3	4	5	6	7	8
3.3(0.8)	<4	1.0(0.4)	<4	<4	<4
1.6(0.3)	1.3(0.3)	<0.9	<0.9	<0.9	<0.9
250	250	350	–	–	–
9	10	11	12	13	14
<4	<4	<4	0.8(0.6)	<4	<4
1.0(0.5)	1.5(0.5)	<0.9	<0.9	1.6(0.30)	<0.9
500	600	–	700	750	–

3.2. The outer face

In Table 1 we present our results along the cone face (i.e. the outer edge of the cone looking down the cone axis towards the nucleus). From this we see the most tentative detections along the face with the strongest occuring (in CO 1 → 0) at positions [24,1], [24,2] and [24,3]. These (especially the latter) correspond to position S1 (Fig. 1), although we see that our 2 → 1 detection is considerably weaker and that both lines are noticeably wider than the detections of Charmandaris et al. (2000). These could, however, be as wide as ∼200 km s^{-1} (at least in CO 2 → 1, Fig. 1), compared to our ≳300 km s^{-1} (Figs. 4 and 5)[4].

[4] Note that like Charmandaris et al. (2000), both transitions, where detected ([24,3]), occur at the same velocity.

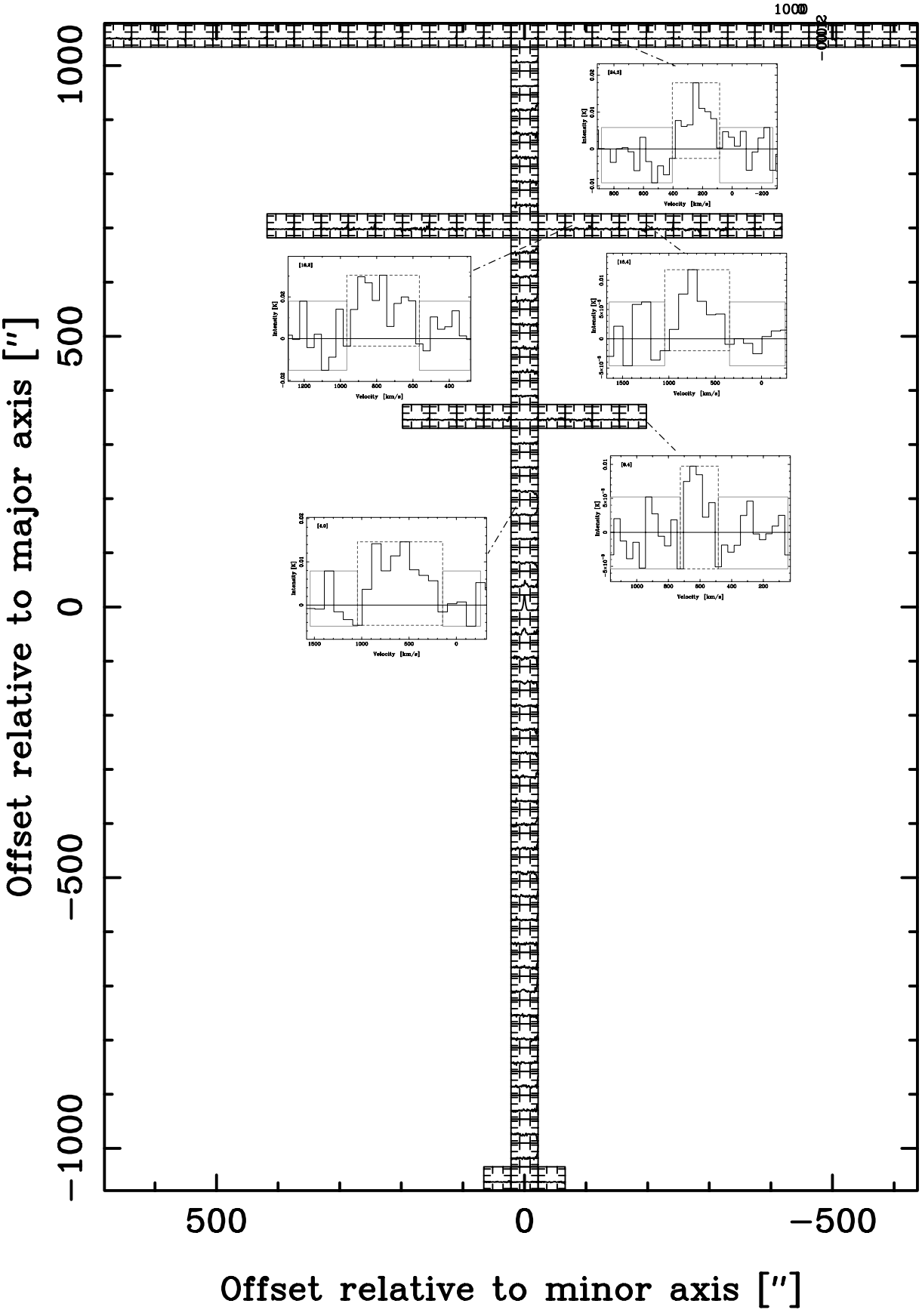

Fig. 4. The full CO 1 → 0 map. "Axis" refers to that of the molecular ring and the insets show the clearest (non-central, see Fig. 6) detections at their respective positions, i.e. at [24,3], [16,2], [16,4], [8,4] and [4,0]. The intensity scale is $T_{\rm A}^{*}$ and the velocities are relative to l.s.r. Except in the cases of [16,4] and [4,0] (100 km s^{-1}), these are shown to a resolution of 40 km s^{-1}. The integrated intensities are given in Tables 1 to 5 and the baseline and moment boxes used to determine these are shown.

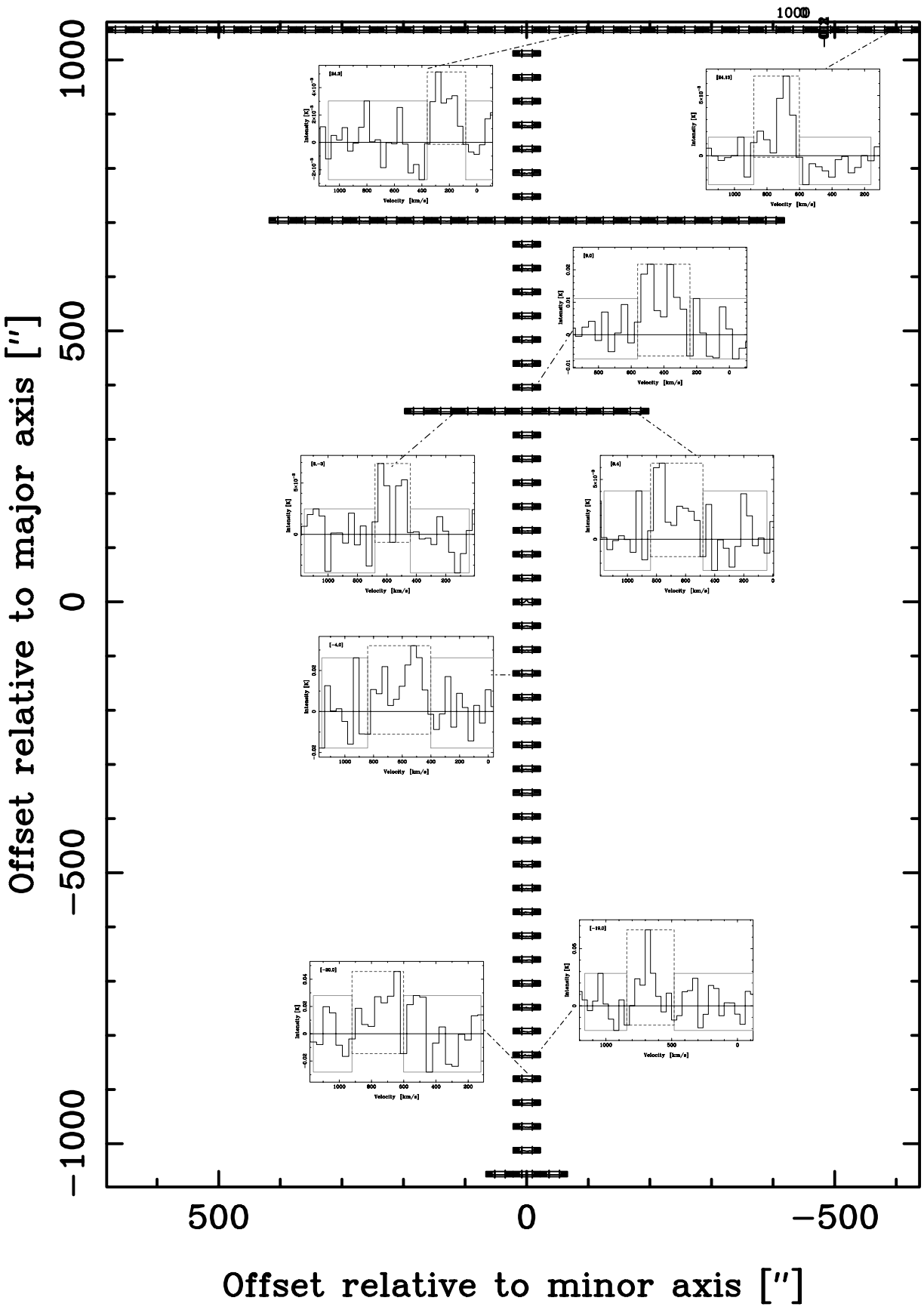

Fig. 5. The full CO 2 → 1 map."Axis" refers to that of the molecular ring and the insets show the clearest (non-central, see Fig. 7) detections at their respective positions, i.e. at [24,3], [24,13], [9,0], [8,−3], [8,4], [−4,0], [−19,0] and [−20,0]. The intensity scale is $T_{\rm A}^{*}$ and the velocities are relative to l.s.r. These are shown to a resolution of 40 km s^{-1}. The integrated intensities are given in Tables 1 to 5 and the baseline and moment boxes used to determine these are shown.

Table 2. The integrated main-beam line intensities at various offsets along the inner jet axis (Fig. 3). As in Table 1, the CO $1 \rightarrow 0$ and $2 \rightarrow 1$ values along with the approximate central velocity are given. See Figs. 6 and 7 for the close-to-central positions [1,0], [0,0] and [−1,0].

	$1 \rightarrow 0$	$2 \rightarrow 1$	vel.		$1 \rightarrow 0$	$2 \rightarrow 1$	vel.
23	2(1)	<2	500	−2	<20	<7	–
22	3.6(1.0)	<2	500	−3	<20	7(3)	600
21	<22	<6	–	−4	<20	12(3)	550
20	<16	<6	–	−5	<20	9(4)	500
19	<16	<6	–	−6	6(2)	<5	550
18	<16	<6	–	−7	6(2)	∼4	700
17	<16	<6	–	−8	<10	<4	–
16	<2	<1	–	−9	5(2)	<6	700
15	<2	<1	–	−10	6(2)	<7	700
14	<15	<7	–	−11	<16	<7	–
13	<15	<7	–	−12	6(2)	<7	700
12	<15	<7	–	−13	<18	9(5)	700
11	4(3)	6(2)	550	−14	<18	<7	–
10	<16	<6	–	−15	5(2)	<7	700
9	<12	7(2)	400	−16	7(2)	5(2)	600
8	0.7(0.3)	<1	450	−17	<12	<7	–
7	2(1)	<4	500	−18	4(2)	<7	600
6	<10	<4	–	−19	5(2)	11(3)	650
5	<10	4(2)	600	−20	<14	12(4)	650
4	10(2)	3(2)	600	−21	5(2)	<7	650
3	5(2)	<4	500	−22	<22	<7	–
2	<10	<4	–	−23	<14	<7	–

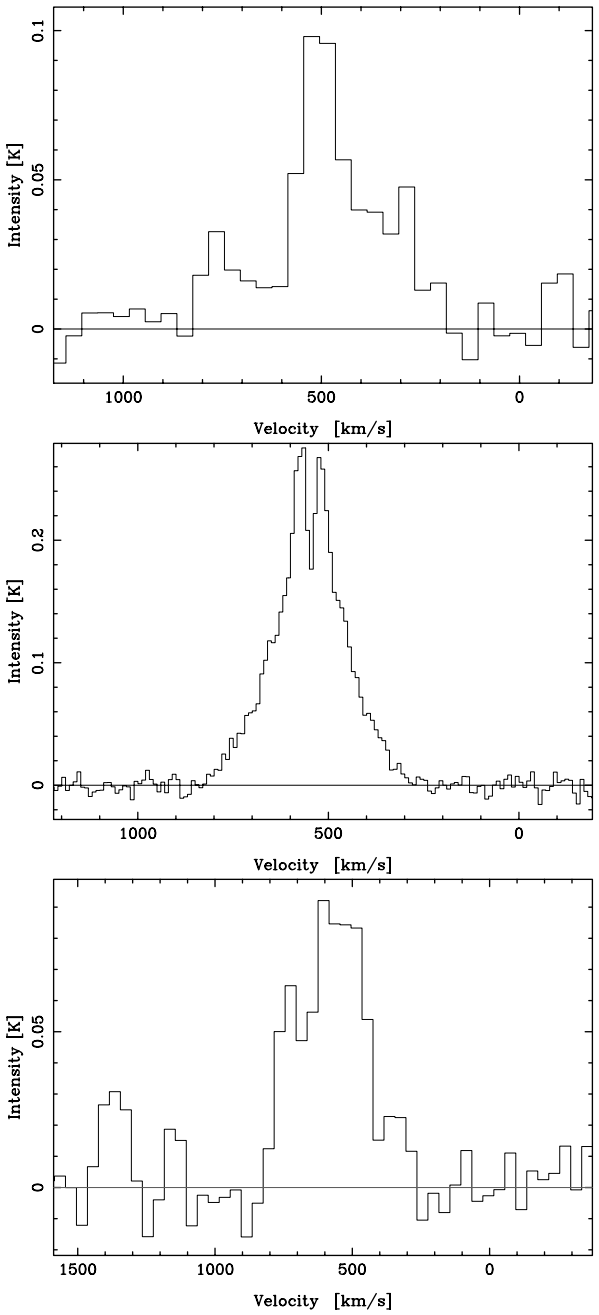

Fig. 6. CO $1 \rightarrow 0$ map at positions [1,0], [0,0] and [−1,0], top, middle and bottom, respectively. The intensity scale is $T_{\rm A}^{*}$ and the central velocities (the scale is shown at of resolutions 40, 10 and 40 km s^{-1}), relative to l.s.r., are 490, 550 (the systemic velocity) and 590 km s^{-1}, respectively. The corresponding integrated main-beam intensities (see Table 1) are 30(2), 77(1) and 39(3) K km s^{-1}, respectively. The centre profile here and in Fig. 7 compare very well with those in Fig. 2 of Israel (1992).

In fact for all of our "detections" the lines are this wide[5], which could result from a range of projected outflow velocities due to the fact that, even in the approaching NE cone, we would have both approaching and receding gas along the line-of-sight through the cone (Curran et al. 1999). What is unusual, however, is the various central velocities along the face, i.e. ≈700 km s^{-1} at the extreme "left" edge ([24,−15], Fig. 3) position falling to lower velocities within this before reaching a minimum (similar to the observed blue-shifts of Charmandaris et al. 2000) before rising again. So although a symmetrical velocity structure along the face is suggested, note that, apart from the centre positions ([24,1] to [24,4]), the detections do require confirmation (Sect. 4).

3.3. The inner jet axis

In Table 2 we show the results along the inner jet axis. Many of these are somewhat noisier (e.g. [18,0]) as a larger proportion of the time was spent on the (edges of the) perpendicular strip positions (Tables 1 and 3). From the table we see a tentative increase in the CO $2 \rightarrow 1/1 \rightarrow 0$ integrated intensity ratio with proximity to the nucleus[6] (where it peaks, Figs. 6 and 7), and although we may

[5] With possible shell structures, tentatively apparent in the $2 \rightarrow 1$ spectra i.e. positions [9,0], [8,−3], [−4,0] and [−20,0], Fig. 5.

[6] As well as a more consistent velocity structure than the outer face (Sect. 3.2).

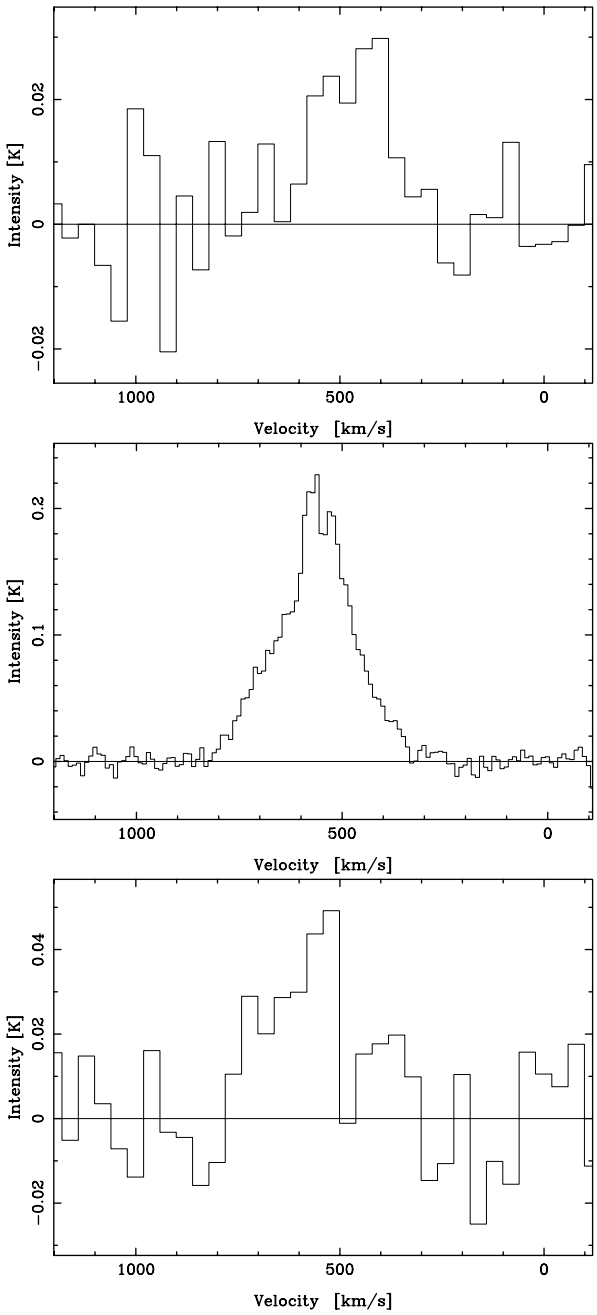

Fig. 7. CO 2 → 1 map at positions [1,0], [0,0] and [−1,0], top, middle and bottom, respectively. As Fig. 6 with integrated main-beam intensities of 11(4), 89(1) and 20(4) K km s^{-1}.

not trust the "detections" in Table 1, we obtain significant ($\gtrsim 2\sigma$) detections in both transitions at position [4,0], corresponding to 3 kpc out along the axis. Also at [9,0] (6 kpc), [−19,0] and [−20,0] (i.e. out to 13 kpc) we may detect CO 2 → 1 at $\gtrsim 2\sigma$, although again the latter two of these is rather tentative (Fig. 5). However, even the distance of the former is much larger than the ∼0.2 kpc radius of the molecular ring (Rydbeck et al. 1993) or the dust lane which crosses Centaurus A (visible in Fig. 1a), suggesting a possible kpc-scale outflow. In addition to this, CO is clearly detected at ±600 pc along

Table 3. The integrated main-beam line intensities at various offsets along row 16 of the map (Fig. 3). See Table 2 for the zero (inner jet axis) position.

−9	−8	−7	−6	−5	−4
<4	1.0(0.5)	5(2)	<12	<8	6(3)
<0.9	∼0.5	<5	<5	<2	4(2)
–	200	500	–	–	550
−3	−2	−1	1	2	3
<10	3(2)	<2	3(1)	10(2)	4(2)
<5	<5	<1	<1	<4	<5
–	600	–	750	750	600
4	5	6	7	8	9
4(1)	<14	<7	<15	1.0(0.7)	2(1)
<5	<5	<5	<5	<1	<1
600	–	–	–	500	500

the inner jet axis[7] (Figs. 6 and 7): Being at a distance of one 1 → 0 beam, we expect negligible smearing of the central CO ring which could cause apparent emission in these positions (Fig. 1c). Notice also from these figures the complex structure of the central ([0,0]) spectra: From the outflow modelling of Curran (2000b)[8], the split peak suggests a ring of inclination[9] ≈20° − 60° and the wings a close to edge-on outflow.

3.4. The remaining strips

In Table 3 the results along the second strip (about position [16,0]) are given. Here we may see a more consistent velocity structure than the outer strip (Table 1), with the maximum being located close to the inner jet axis. Again this is possibly symmetrical with the lower velocities occuring towards the edges, although, again this is tentative and so requires confirmation. Only two significant detections were obtained (in 1 → 0) at [16,2] and [16,4] (Fig. 4), the strongest of which (the former) extrapolates from the centre to [24,3], which is the location of our strongest outer strip detection (S1 of Fig. 1, see Fig. 3 and Sect. 3.2).

In Table 4 we show the results along the inner strip (about position [8,0]). From this we have 2 significant detections: CO 2 → 1 at [8,−3] and both transitions at [8,4], Figs. 4 and 5. The former position extrapolates to [24,−8] on the outer strip, where we have tentative detections, and

[7] This is very reminiscent of the situation in Circinus and is discussed in Sect. 3.5.

[8] Further examples may be seen in Curran et al. (1999) and Curran (1998, 2000a).

[9] Defined relative to the sky plane, i.e. an edge-on ring would have an inclination of 90° (Curran 1998).

Table 4. The integrated main-beam line intensities at various offsets along row 8 of the map (Fig. 3). See Table 2 for the zero (inner jet axis) position.

−4	−3	−2	−1
<4	<4	5(2)	<4
<1	1.5(0.3)	<4	<4
–	550	650	–
1	2	3	4
<10	<10	<6	1.3(0.50)
4(2)	4(2)	<1	1.4(0.5)
600	600	–	600

Table 5. The integrated main-beam line intensities at various offsets along row −24 of the map (Fig. 3).

−1	0	1
0.9(0.5)	<6	<3
<1	<1	<1
500	–	–

the latter to [24,13], where we have a significant $2 \rightarrow 1$ detection (Table 1 and Fig. 5). By means of pure speculation, if positions [24,−8] and [24,13] signify the outer edge of a cone, this would give it an opening angle of ≈50° (cf. $60 \pm 10°$ for the ionisation cone, Bryant & Hunstead 1999, see Sect. 3.5) with its axis displaced by ≈5° from the jet axis, i.e. passing through [16,2] and [24,3], where we have our strongest and most convincing strip detections (Tables 1 and 3 and Figs. 4 and 5). This "cone" is traced upon the map in Fig. 3. Looking at Fig. 1, we see that the position angle of 51° only applies to the inner ∼3 kpc of the jet (e.g. Israel 1998) which would place [24,3] closer to S1 than [24,0].

In Table 5 the SW outer face (about [−24,0]) is shown. We did not obtain any significant detections here but, as explained in Sect. 3.1, this is not so surprising due to the kink in the radio lobe axis (Fig. 1 and e.g. Israel 1998).

3.5. Discussion

A signature of Seyfert nuclei is the presence of ionised gas along the radio jets present in active galactic nuclei (e.g. Begelman et al. 1984; Schulz 1988; Colbert et al. 1996, 1998). The ionised material and the observed photons are collimated by the dusty material ("torus") obscuring the continuum source (Antonucci & Miller 1985; Wilson et al. 1988; Tadhunter & Tsvetanov 1989; Wilson & Tsvetanov 1994; Baker & Scoville 1998), causing them to exhibit a sharp linear edge so that the ionised gas is observed as a full cone in the narrow line region (Storchi-Bergmann & Bonatto 1991; Storchi-Bergmann et al. 1992; Dopita et al. 1998). In this model, ionised gas which passes through the sublimation radius (where hot dust radiates in the infrared) is broken into clouds which are able to fall back closer to the nucleus, possibly being observed as the broad line region (e.g. Antonucci & Miller 1985; Krolik & Begelman 1986; Miller et al. 1991; Heisler et al. 1997). Dust and ionised gas which have accreted onto the AGN are driven back outward in the direction of the jets by radiation pressure, thus maintaining the direction of the jet flow (Wilson & Tsvetanov 1994; Capetti et al. 1996). Ionisation cones are expected to have a dusty layer form along their inner edge (Dopita et al. 1998), thus permitting the presence of molecules along the surface of the outflow. In the model of Dopita et al. (1998), the ionisation cone and the radio jet have different origins, i.e. from the dusty torus[10] and from the black hole, respectively (Whittle et al. 1988). It should be noted, however, that the generally small scales and wide opening angles of the cones, in comparison with the jets, can also be explained by a simple wide ionised outflow in which the radio jet is simply a central high velocity component (Wilson et al. 1993). In Circinus the radio jets close to the nucleus have been inferred from the observations of Davies et al. (1998)[11] and the ionisation cone in the form of a unipolar (to the north-west only) V-shaped outflow, Fig. 2. The highly ionised state of the highly excited (Oliva et al. 1994) low density ($n_e \sim 40$ cm^{-3}, Marconi et al. 1994) supersonic (Veilleux & Bland-Hawthorn 1997) gas is confirmed by the presence of the [NeIII, V, VI], [SIV], [MgV,VII,VIII], [OIV] and [SiIX] species (Moorwood et al. 1996). The various outflow features in Circinus are summarised in Table 6, and the results appear to support the hypothesis that the jet drives the ionisation cone, together with an envelope of molecular gas, out along the rotation axis of the molecular ring (Curran et al. 1998, 1999, Fig. 2). Returning to Sect. 1, it does not seem unfeasible that the findings of Charmandaris et al. (2000) may be due to a similar situation in Centaurus A[12]: Note that Bryant & Hunstead (1999) obtain the same position angle as for the radio jet axis. In this galaxy, the CO detections also appear to associated with HI clumps (Schiminovich et al. 1994) and although in Circinus HI has been detected out to nearly 100 kpc (Jones et al. 1999) in a complex spiral/bar structure, it is unclear how this is related to the ≲kpc-scale molecular outflow.

[10] Pedlar et al. (1998) propose a model where the torus is a consequence of the weak radiation emitting from the equator of the continuum source, whereas the cone arises from gas ionised by the strong polar radiation.

[11] Elmouttie et al. (1995) also observe large-scale radio lobes.

[12] Note that although the "shells" lie at much greater distances than the Circinus cone faces, ionisation cones on scales of 100 pc–18 kpc have been observed in Seyfert galaxies (e.g. Ulvestad & Wilson 1984; Wilson & Tsvetanov 1994; Sandqvist et al. 1995; Christopoulou et al. 1997; Su et al. 1996; Márquez et al. 1998).

Table 6. The outflow properties in Circinus. The Hα outflow (Elmouttie et al. 1998) is observed towards the NW only. *Note that Veilleux & Bland-Hawthorn (1997) (also) derive a position angle of $\approx$295° but an opening angle of $\sim$100° for the ionised outflow. In the case of the radio continuum (Harnett et al. 1990; Elmouttie et al. 1995) and CO (Curran et al. 1999) observations, outflows are also detected towards the SE, although, unlike the molecular outflow, the radio lobe is strongest in the NW.

	Radio	Hα	CO
Position angle	$\approx$115° and $\approx$315°	$292 \pm 5°$*	120° and $300 \pm 20°$
Inclination angle	–	-90 to 40°	$-12°$ and $168 \pm 10°$
Opening angle	15°	66°*	$90 \pm 5°$
Inferred length	$\pm$1 kpc	400 to 520 pc	$\approx \pm 500$ pc
Outflow velocity	–	150 to 200 km s^{-1}	$\leq 190 \pm 10$ km s^{-1}

Also in Seyfert galaxies, the inflow of gas in the galaxy results in the molecular ring, located at the inner Lindblad resonance (as in point 2 of Sect. 1), from which gas may somehow be accreted to the central super-massive black hole[13] powering the Seyfert activity (see Curran 2000b, for a review)[14]. As mentioned, in Circinus the 100 pc-scale molecular ring is found to be aligned perpendicular to the jet/outflow thus suggesting that it is coplanar with the small-scale ($\sim$pc) torus responsible for the obscuration of the broad line regions in type 2 Seyferts (Antonucci & Miller 1985; Antonucci 1993)[15]. Returning to Sect. 3.3, while we estimate quite a low inclination, Rydbeck et al. (1993) *assume* an inclination of close to 90° for the molecular ring which is similar to the $\approx$80° modelled for the torus (Bryant & Hunstead 1999). Our discrepancy could be due to a misalignment between ring and torus or perhaps the peak in Figs. 6 and 7 arises from another source, e.g. the dust lane, with the wings being due to the molecular ring (Israel 1992). Note, however, that Skibo et al. (1994) derive an X-ray jet sky plane inclination of $\approx$30° which would give an inclination of $\approx$60° to a perpendicular ring, thus agreeing better with our estimate. This jet is believed to be coincident with the radio jet out to 10–20 kpc although it should be kept in mind that this has been observed to bend significantly both on the large (Sect. 3.1) and small-scale (by as much as 60° on the sub-pc scale, Fujisawa et al. 2000).

It is most likely that both of these models are gross oversimplifications (at least we consider ours to be), although, unlike Israel (1992), ours does provide an explanation for the split peak (Fig. 6 and 7). In order to resolve this further observations are certainly required (next section).

4. Summary

We have performed a partial large-scale map along the North-Eastern quadrant of Centaurus A in the lowest two rotational transitions of CO. From this we obtain some tentative detections at $\gtrsim$kpc distances from the nucleus, and although those located on the most distant mapped strip exhibit similar Doppler shifts as previously (Charmandaris et al. 2000), our lines appear to be significantly wider. Three of the positions located along this strip (i.e. the outer edge of our map) are aligned with better detections from the other inner two map strips, suggesting strong emission emanating from the nucleus along these directions, perhaps signifying the outer edge of a cone (of opening angle $\sim$50° and PA $\approx$ 45°?). Also, many of the "detections" suggest a complex dynamical structure, although, until verified, these are too weak to be trusted[16]. Even though our results for these outer positions hardly fill us with confidence, and keeping in mind that the detections of Charmandaris et al. (2000), from which they deduce the presence of molecular shells are only at a 4σ level, we still believe that the presence of a

[13] This has been detected in Centaurus A by Marconi et al. (2001) and inferred in Circinus by e.g. Greenhill (2001).

[14] As well as being common to Seyfert galaxies, similar molecular rings ($\approx$300 to 800 pc) are also observed in ultraluminous infrared galaxies (ULIRGs) (Downes & Solomon 1998; Genzel et al. 1998). These galaxies are so bright in the far-IR (Soifer et al. 1984), that they may host an AGN (possibly a quasar, Sanders et al. 1988) in addition to an extreme star-burst (e.g. Solomon et al. 1992).

[15] These may also, in general, tend to be aligned with the galactic disk (Curran et al. 1998; Curran 2000a).

[16] As well as verification of the CO detections, these regions should also be mapped in density tracing molecules, such as HCN and CS, as this would give a clue on the physical conditions of the gas. For example, from such a study, Curran et al. (2001a) suggest that the molecular gas within the central few hundred parsecs of Circinus is distributed in denser clouds than in the otherwise similar NGC 4945. If such "clumpiness" was found in Centaurus A it could explain the inconsistent kinematics of the gas along the jet axis direction. As yet no such observations in this region exist, although along the dust lane (Wild & Eckart 2000), they give HCN to CO ratios which are comparable with ULIRGs (Solomon et al. 1992) and other Seyferts (Curran et al. 2000, 2001b), suggesting that the gas in this region is widely distributed in dense star forming clouds rather than a more diffuse component surrounding the AGN (Wild & Eckart 2000) (see also Curran et al. 2001a).

molecular outflow is a distinct possibility on the grounds that:

1. Charmandaris et al. (2000) only detected CO along the jet direction, thus suggesting a possible relationship between these two phenomena as in the Circinus jet/outflow model.
2. We have clear detections of CO along the inner jet direction at distances which exclude the possibility that the emission arises from the central molecular ring.
3. The wings in the central spectrum may also suggest the presence of an outflow.

If the detections of Charmandaris et al. (2000) were due to a large-scale outflow this could explain the initial presence of molecular gas in these regions[17], which presents a problem for the shell model. However, since their detections appear to be of slightly better quality than ours, we cannot rule out the shell model, at least in addition to a possible small-scale (∼kpc) outflow. The nature of the molecular gas (i.e. HCN *as well as* CO) along the jet direction naturally requires much more study[18]: These results were obtained after 70 hours of observation and therefore many hundreds of hours of much over-subscribed SEST time would be required in order to produce a full map to the necessary sensitivity. It is hoped that this paper may be used to justify such a large-scale/long-term project.

Acknowledgements. I would like to thank the referee R. Antonucci for his helpful comments, G. Rydbeck for drawing my attention to the work of Charmandaris et al. (2000) and V. Charmandaris for the preprint and postscript file. Also thanks to Lars E. B. Johansson at Onsala Space Observatory for suggesting the perpendicular strips and Melinda Taylor at the University of New South Wales for her prompt installation of Per Bergman's *xs* data reduction program.

References

Antonucci, R. R. J. 1993, ARA&A, 31, 473
Antonucci, R. R. J., & Miller, J. S. 1985, ApJ, 297, 621
Baker, A. J., & Scoville, N. Z. 1998, Am. Astron. Soc. Meet., 192, 3605
Begelman, M. C., Blandford, R. D., & Rees, M. J. 1984, Rev. Mod. Phys., 56, 255
Bryant, J. J., & Hunstead, R. W. 1999, MNRAS, 308, 431
Burns, J. O., Feigelson, E. D., & Schreier, E. D. 1983, ApJ, 273, 128
Capetti, A., Axon, D. J., Macchetto, F., Sparks, W. B., & Boksenberg, A. 1996, ApJ, 469, 554
Charmandaris, V., Combes, F., & van der Hulst, J. M. 2000, A&A, 356, L1
Christopoulou, P. E., Holloway, A. J., Steffen, W., et al. 1997, MNRAS, 284, 385
Clarke, D. A., Burns, J. O., & Norman, M. L. 1992, ApJ, 395, 444
Colbert, E. J. M., Baum, S. A., Gallimore, J. F., O'Dea, C. P., & Christensen, J. A. 1996, ApJ, 467, 551
Colbert, E. J. M., Baum, S. A., O'Dea, C. P., & Veilleux, S. 1998, ApJ, 496, 786
Curran, S. J. 1998, Licentiate Thesis, Chalmers University of Technology
Curran, S. J. 2000a, A&AS, 144, 271
Curran, S. J. 2000b, Ph.D. Thesis, Chalmers University of Technology
Curran, S. J., Aalto, S., & Booth, R. S. 2000, A&AS, 141, 193
Curran, S. J., Johansson, L. E. B., Bergman, P., Heikkilä, A., & Aalto, S. 2001a, A&A, 367, 457
Curran, S. J., Johansson, L. E. B., Rydbeck, G., & Booth, R. S. 1998, A&A, 338, 863
Curran, S. J., Polatidis, A. G., Aalto, S., & Booth, R. S. 2001b, A&A, 368, 824
Curran, S. J., Rydbeck, G., Johansson, L. E. B., & Booth, R. S. 1999, A&A, 344, 767
Davies, R. I., Forbes, D. A., Ryder, S., et al. 1998, MNRAS, 293, 189
Dopita, M. A., Heisler, C., Lumsden, S., & Bailey, J. 1998, ApJ, 498, 570
Downes, D., & Solomon, P. M. 1998, ApJ, 507, 615
Elmouttie, M., Haynes, R. F., Jones, K. L., et al. 1995, MNRAS, 275, L53
Elmouttie, M., Koribalski, B., Gordon, S., et al. 1998, MNRAS, 297, 49
Fujisawa, K., Inoue, M., Kobayashi, H., et al. 2000, PASJ, 52, 1021
Genzel, R., Lutz, D., Sturm, E., et al. 1998, ApJ, 498, 579
Greenhill, L. J. 2001, in Proceedings of the 5th EVN Symposium, ed. J. Conway, A. Polatidis, & R. Booth (Göteborg, Sweden: Chalmers University of Technology), 101
Harnett, J. I., Whiteoak, J. B., Reynolds, J. E., Gardner, F. F., & Tzioumis, A. 1990, MNRAS, 244, 130
Heisler, C. A., Lumsden, S. L., & Bailey, J. A. 1997, Nature, 385, 700
Irwin, J. A., & Sofue, Y. 1992, ApJ, 396, L75
Israel, F. P. 1992, A&A, 265, 487
Israel, F. P. 1998, A&AR, 8, 237
Jones, K. L., Koribalski, B. S., Elmouttie, M., & Haynes, R. F. 1999, MNRAS, 302, 649
Krolik, J. H., & Begelman, M. C. 1986, ApJ, 308, L55
Marconi, A., Capetti, A., Axon, D., et al. 2001, ApJ, 549, 915
Marconi, A., Moorwood, A. F. M., Origlia, L., & Oliva, E. 1994, ESO Messenger, 78, 20
Márquez, I., Boisson, C., Durret, F., & Petitjean, P. 1998, A&A, 333, 459
Miller, J. S., Goodrich, R. W., & Mathews, W. G. 1991, ApJ, 378, 47
Moorwood, A. F. M., Lutz, D., Oliva, E., et al. 1996, A&A, 315, L109
Oliva, E., Salvati, M., Moorwood, A. F. M., & Marconi, A. 1994, A&A, 288, 457
Pedlar, A., Fernandez, B., Hamilton, N. G., Redman, M. P., & Dewdney, P. E. 1998, MNRAS, 300, 1071
Phillips, M. M., Jenkins, C. R., Dopita, M. A., Sadler, E. M., & Binette, L. 1986, AJ, 91, 1062
Rydbeck, G., Wiklind, T., Cameron, M., et al. 1993, A&A, 270, L13

[17] Perhaps arising from the jets shocking the inter-galactic medium or the recombination of ionised gas.

[18] If the features are found to be due to an outflow this would the third Seyfert in which such an outflow is detected (Irwin & Sofue 1992; Curran et al. 1999).

Sanders, D. B., Soifer, B. T., Elias, J. H., Neugebauer, G., & Matthews, K. 1988, ApJ, 328, L35
Sandqvist, A., Jörsäter, S., & Lindblad, P. 1995, A&A, 295, 585
Schiminovich, D., van Gorkom, J. H., van der Hulst, J. M., & Kasow, S. 1994, ApJ, 423, L101
Schulz, H. 1988, A&A, 203, 233
Skibo, J. B., Dermer, C. D., & Kinzer, R. L. 1994, ApJ, 426, L23
Soifer, B. T., Rowan-Robinson, M., Houck, J. R., et al. 1984, ApJ, 278, L71
Solomon, P. M., Downes, D., & Radford, S. J. E. 1992, ApJ, 387, L55
Storchi-Bergmann, T., & Bonatto, C. J. 1991, MNRAS, 250, 138
Storchi-Bergmann, T., Wilson, A. S., & Baldwin, J. A. 1992, ApJ, 396, 45
Su, B. M., Muxlow, T. W. B., Pedlar, A., et al. 1996, MNRAS, 279, 1111
Tadhunter, C., & Tsvetanov, Z. 1989, Nature, 341, 422
Ulvestad, J. S., & Wilson, A. S. 1984, ApJ, 285, 439
Veilleux, S., & Bland-Hawthorn, J. 1997, ApJ, 479, L105
Whittle, M., Pedlar, A., Meurs, E. J. A., et al. 1988, ApJ, 326, 125
Wild, W., & Eckart, A. 2000, A&A, 359, 483
Wilson, A. S., Braatz, J. A., Heckman, T. M., Krolik, J. H., & Miley, G. 1993, ApJ, 419, L61
Wilson, A. S., & Tsvetanov, Z. I. 1994, AJ, 107, 1227
Wilson, A. S., Ward, M. J., & Haniff, C. A. 1988, ApJ, 334, 121